Dispersionless Flat Mode and Vibrational Anomaly in Active Brownian Vibrators Induced by String-like Dynamical Defects

Cunyuan Jiang[1,2,3], Zihan Zheng[1,4], Yangrui Chen[1,4], Matteo Baggioli[1,2,3],* and Jie Zhang[1,4]†
[1] *School of Physics and Astronomy, Shanghai Jiao Tong University, Shanghai 200240, China*
[2] *Wilczek Quantum Center, School of Physics and Astronomy, Shanghai Jiao Tong University, Shanghai 200240, China*
[3] *Shanghai Research Center for Quantum Sciences, Shanghai 201315,China and*
[4] *Institute of Natural Sciences, Shanghai Jiao Tong University, Shanghai 200240, China*

In recent years, active Brownian particles have emerged as a prominent model system for comprehending the behaviors of active matter, wherein particles demonstrate self-propelled motion by harnessing energy from the surrounding environment. A fundamental objective of studying active matter is to elucidate the physical mechanisms underlying its collective behaviors. Drawing inspiration from advancements in molecular glasses, our study unveils a low-energy "flat mode" within the transverse spectrum of active Brownian vibrators – a nearly two-dimensional, bi-disperse granular assembly. We demonstrate that this collective excitation induces an anomalous excess in the vibrational density of states (VDOS) beyond the phononic Debye contribution. Additionally, we establish through empirical evidence that string-like dynamical defects, discerned via the spatial distribution of each particle's contribution to the reduced transverse VDOS, serve as the microscopic origin of the flat mode and its associated anomalies. These findings underscore the pivotal role of string-like dynamical defects in elucidating the vibrational and mechanical properties of active Brownian particles.

Introduction – Active Brownian particles have recently gained popularity as a modeling system for investigating microorganisms such as bacteria, cells, and microswimmers [1–9]. Unlike passive Brownian particles, active Brownian particles do not exist in thermal equilibrium; they exhibit self-propelled motion by harnessing energy from their surrounding environment [1, 2]. Understanding the behavior of these active particles is crucial for deciphering processes like cell migration in intricate tissue and organ formation [1], as well as wound healing [10]. Furthermore, a deeper understanding of active Brownian particles is imperative for the development of artificial micro- and nanorobots intended for future applications in drug delivery and environmental protection.

Chen et al. recently conducted an experiment involving a quasi-two-dimensional granular system of uniformly driven active Brownian vibrators [11, 12]. In this system, the statistics of single-particle velocity and rotation adhere to Gaussian distributions with zero means [11]. This experimental setup closely mirrors the active Brownian particles scrutinized in theoretical studies, as it lacks inherent particle-scale alignment interactions [8]. The system comprises numerous hard-disk-like particles, each devoid of any inherent orientation in shape and without preferred translational or rotational directions, owing to the absence of sub-particle scale built-in asymmetries, in contrast to the earlier studies [13–16]. Unlike microswimmers, which operate within a viscous and overdamped surrounding medium, the underdamped dynamics observed in this system offer a convenient experimental platform. This platform allows for the direct observation and analysis of collective shear excitations in bi-disperse systems [17], all while mitigating issues associated with crystallization.

In our surroundings, amorphous soft matter systems, including gels, structural glasses, colloids, and granular assemblies, are commonplace. However, their dynamic, thermodynamic, and mechanical properties remain poorly understood in contrast to the well-explained behaviors of ideal crystals, predominantly governed by elastic theory and harmonic lattice vibrations (phonons) [18]. These soft matter systems exhibit non-phononic degrees of freedom, collectively termed as 'defects,' which contribute to the observed anomalies alongside crystal-like acoustic waves. Within amorphous materials, the concept of 'defects' manifests in various forms. For instance, they are recognized as two-level systems [19, 20] elucidating the low-temperature heat capacity [21], quasilocalized non-phononic modes [22] accounting for the boson peak (BP) excess in the vibrational density of states [23], and as entities such as shear transformation zones [24], Eshelby quadrupoles [25], or topological defects [26], providing insight into mechanical and plastic dynamics during deformation [27].

In recent studies, there has been a notable focus on the significance of string-like dynamical defects across a spectrum of materials, including supercooled liquids, heated crystals, quasi-crystals, and glasses. These defects bear resemblance to vortex lines observed in superfluids [28] and play a crucial role in shaping relaxational and dynamical properties [29–35]. Simulation-based investigations have revealed that these quasi-one-dimensional entities [36], primarily of transverse nature, emerge as the most plausible candidates responsible for the manifestation of nonphononic modes. It is furthermore postulated that these string-like excitations serve as a microscopic origin of the boson peak (BP) phenomenon typical of glassy materials [37–43]. Of particular interest are findings from simulations by Hu and Tanaka [38, 39], which establish a close correlation between these string-like excitations and the emergence of a "flat boson peak mode". This mode, characterized by collective and dispersionless low-energy excitation, has also been observed in experimental studies on the boson peak within two-dimensional amorphous materials [44]. Despite accumulating experimental evidence in various amorphous systems [45–47], direct experimental validation of dynamical string-like defects in amorphous active Brownian particles remains elusive. Enhanced understanding of vibrational and collective dynamics in these particles holds promise in elucidating fundamental characteristics pertaining to the mechanics and hydrodynamics of active matter [1, 48].

In this study, we have uncovered a distinctive mode within the low-frequency spectrum of a two-dimensional layer comprising bi-disperse active Brownian vibrators through an analysis of their dynamic matrices. Termed the 'dispersionless flat mode', this transverse mode manifests as an anomalous augmentation in the vibrational density of states (VDOS) beyond the typical phononic Debye contribution. Through a detailed examination of the VDOS at the particle level, we have pinpointed the microstructural origin of this flat mode and its associated anomalies: the string-like excitation within the spectral domain. Notably, our discovery corroborates recent theoretical propositions by Hu and Tanaka [38, 39], despite the substantial distinctions between our active Brownian particle system and conventional molecular glasses.

Experimental setup and data analysis – Our experimental system consists in a horizontal layer of granular particles driven vertically by a sinusoidal oscillation with a fixed frequency of 100 Hz and amplitude of 0.062 mm induced by an electromagnetic shaker. To prevent crystallization, we utilize bi-disperse particles with a size ratio of disk diameters of 1:1.4 and a number ratio of 2:1 for small and large. The total particle number is 798 with packing fraction $\phi = 0.822$. The motion of the particles, labeled "granular Brownian vibrators", is recorded with a Basler CCD camera (acA2040-180kc) at 40 frames/s for at least an hour. We refer to Refs. [11, 17] for more details about the experimental setup.

The analysis of the experimental data is based on the displacement correlation matrix $\boldsymbol{C}$, defined as [49, 50]

$$C_{ij} = \langle n(t)_i n(t)_j \rangle_T, \tag{1}$$

where $n_i(t)$ is the displacement of ith degree of freedom at time t, and T the time window on which the average $\langle \cdot \rangle$ is performed. The dynamical matrix can then be calculated as,

$$D_{ij} = \frac{\alpha\, C_{ij}^{-1}}{\sqrt{m_i m_j}}, \tag{2}$$

where m_i is the mass of the ith degree of freedom, and α is a dimensionful parameter which is fixed using the same procedure outlined in [17]. By diagonalizing the matrix $\boldsymbol{D}$, one obtains the eigenvalues κ_i and the eigenfrequencies $\omega_i = \sqrt{\kappa_i}$. The eigenvector fields $\boldsymbol{u}$ are then defined by solving the eigenvalue problem, $\boldsymbol{D}\boldsymbol{u} = \omega^2 \boldsymbol{u}$. From the eigenvector field $\boldsymbol{u}$, longitudinal (L) and transverse (T) dynamical structure factor are extracted,

$$S_{L,T}(\boldsymbol{k},\omega) \propto \frac{1}{k^2} \left| \sum_i F_{(L,T),i}(\boldsymbol{k}) \delta_{\omega,\omega_i} \right|^2, \tag{3}$$

with

$$F_{L,i}(\boldsymbol{k}) = \boldsymbol{k} \cdot \sum_j \boldsymbol{u}_i(\boldsymbol{r}_j) e^{-i\boldsymbol{k}\cdot\boldsymbol{r}_j}, \tag{4}$$

$$F_{T,i}(\boldsymbol{k}) = \boldsymbol{z} \cdot \boldsymbol{k} \times \sum_j \boldsymbol{u}_i(\boldsymbol{r}_j) e^{-i\boldsymbol{k}\cdot\boldsymbol{r}_j}. \tag{5}$$

Here, $\boldsymbol{z}$ is the vector perpendicular to the two-dimensional experiment platform, while the index j runs over all particles and $\boldsymbol{r}_j$ is the position of jth particle. The vibrational density of states (VDOS) can be obtained by $g(\omega) = \sum_i \delta_{\omega,\omega_i}$, or equivalently $g(\omega)_{L,T} = \int S_{L,T}(\boldsymbol{k},\omega) d\boldsymbol{k}$, showing perfect agreement. Finally, the particle level VDOS is given by $g_{L,T}(\boldsymbol{r}_j,\omega) = \sum_i |\boldsymbol{u}_{i,L,T}(\boldsymbol{r}_j)|^2 \delta_{\omega,\omega_i}$ where $\boldsymbol{u}_{i,L,T}(\boldsymbol{r}_j)$ is the longitudinal or transverse eigenvector field of jth particle under eigenfrequency ω_i [38, 39].

Dynamical response and vibrational anomalies – The transverse dynamical structure factor is shown as a functon of frequency and for different wave-vectors in Fig.1. The experimental data are visualized with red symbols. The thick red lines are the results of a fit with the following function,

$$S_T(\omega,k) \propto \frac{\omega^2}{(\omega^2 - \Omega_T^2)^2 + \omega^2 \Gamma_T^2} + S_{\text{extra}}(\omega). \tag{6}$$

with

$$S_{\text{extra}}(\omega) = \frac{1}{\omega\sigma\sqrt{2\pi}} \exp\left(-\frac{(\ln\omega - \mu)^2}{2\sigma^2}\right), \tag{7}$$

while the thin lines are the two contributions in Eq. (6). The first term corresponds to a damped harmonic oscillator with linewidth $\Gamma_T(k)$ and characteristic frequency $\Omega_T(k)$. The second term represents a log-normal function [51] that describes additional low-energy modes as commonly utilized in amorphous systems [38, 39].

The results of Fig.1 outline the presence of two distinct excitations, captured by the two terms in Eq.(6). The first mode, whose dispersion $\Omega_T(k)$ is indicated with a black dashed line, corresponds to propagating shear waves (transverse phonons) with a speed of $v_T = 71.7$ d_s/s (in unit of the small particle diameter d_s). At this specific value of the packing fraction, the system is in a dense liquid state and the collective shear waves present a small gap in wave-vector [17], known as k-gap [52], that emerges nevertheless at smaller wave-vector and is not shown in Fig.1.

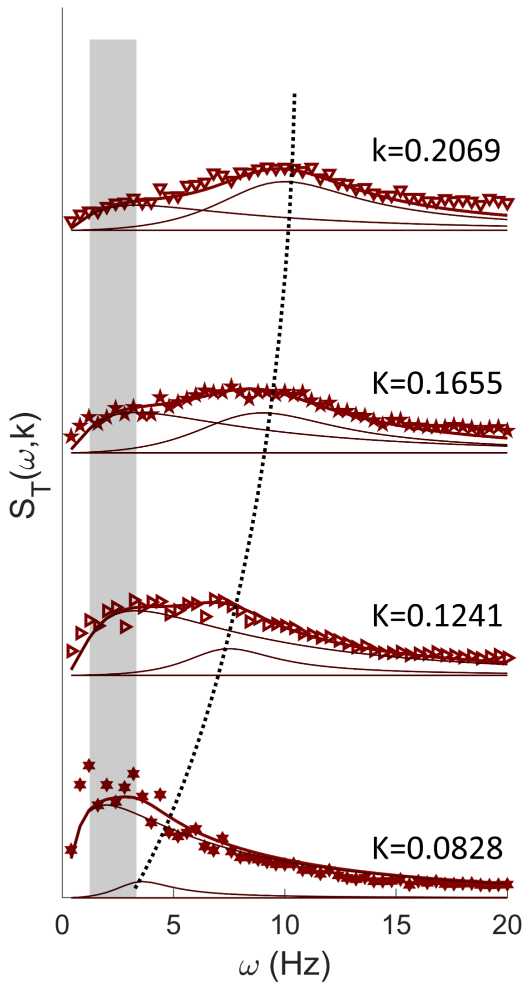

FIG. 1: The transverse dynamical structure factor $S_T(\omega, k)$. The red symbols are the experimental data. The solid lines represent the fit using Eq.(6). The dashed line marks the dispersion of the transverse phonon mode $\Omega_T(k)$, while the gray vertical region indicates the energy of the dispersionless flat mode plus/minus its uncertainty.

The second excitation appears at frequencies below those of the transverse phonon and corresponds to the peak whose position is highlighted by the vertical gray area. Interestingly, we find that the energy of this collective mode does not depend on the wave-vector k. Hence, we label this excitation the "dispersionless flat mode" (DFM). As the wave-vector becomes larger, the intensity of the peak associated to the DFM becomes weaker with respect to that of the concomitant transverse phonon.

Importantly, a DFM can only be found in the transverse dynamical structure factor, indicating its transverse nature. As demonstrated in the Supplementary Information (SI), the longitudinal dynamical structure factor $S_L(\omega, k)$ displays a single peak, corresponding to a longitudinal phonon mode with linear dispersion relation, $\Omega_L(k) = v_L k$, and speed $v_L = 116.9$ d$_s$/s [17].

In order to confirm the existence of the DFM and study its impact on the vibrational properties of our system, we move to the analysis of the VDOS, $g(\omega)$. To better visualize our results, we normalize the VDOS by the two-dimensional Debye scaling $g_{\text{Debye}} \propto \omega$. Our experimental results are shown in Fig.2, where the blue, red and gray lines correspond respectively to the longitudinal, transverse and total density of states.

At low frequency, the longitudinal part of the VDOS is approximately constant, indicating the validity of the Debye approximation, and consistent with the observation of a linearly dispersing longitudinal phonon. It then shows a pseudo-Van Hove peak at approximately 12 Hz, that agrees with the energy at which $\Omega_L(k)$ flattens (see SI), and then decays at higher frequencies, vanishing above ≈ 30 Hz.

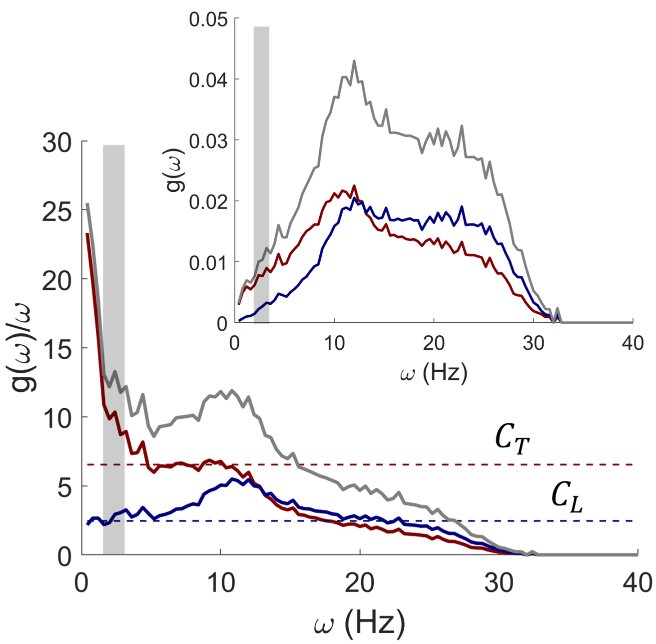

FIG. 2: The reduced VDOS for packing fraction $\phi = 0.822$. The inset shows the original VDOS. The blue, red, and gray colors correspond to the longitudinal, transverse, and total VDOS. The vertical gray area indicates the energy of the dispersionless flat mode observed in the dynamical structure factor, Fig.1. The dashed lines denote the position of the longitudinal and transverse Debye levels, $C_{L,T}$, determined from the corresponding sound speeds.

The transverse component of the VDOS (red curve in Fig.2), presents a more complex behavior that can be divided in three different regions. Below 1 Hz, the transverse VDOS decays monotonically indicating the presence of a strong diffusive component that can be also seen from a large nonzero value of $g_T(\omega)$ at zero frequency (see inset of Fig.2). Above ≈ 3 Hz, the transverse VDOS is similar to the longitudinal one, with the difference that the pseudo-Van Hove peak is much weaker. This indicates that the transverse dynamics are more overdamped than the longitudinal ones. In order to test the validity of Debye theory, we focus on the low frequency range in which the transverse and longitudinal reduced VDOS display an approximate plateau. We mark the corresponding plateaus with horizontal dashed lines in Fig.2. We verify that the ratio of the values of the two plateaus, C_L/C_T, agrees well with the prediction of the Debye model, v_T^2/v_L^2 where the speeds are extracted from the dispersion relations obtained from the dynamical structure factor.

More interestingly, between $\approx$ 1-3 Hz, we observe an excess anomaly in the Debye reduced transverse VDOS whose energy is compatible with the DFM observed in the dynamical structure factor, Fig.1, and whose structure is similar to the boson peak observed in several amorphous materials [23].

The connection between a dispersionless flat mode and the boson peak anomaly has been highlighted in simulations [38, 39] and observed experimentally [44], and its a direct manifestation of the presence of additional (and likely localized) low-energy degrees of freedom responsible for the BP.

String-like dynamical defects – After proving a direct link between the flat mode and the BP excess anomaly in the VDOS, we are now in a position to investigate its microscopic origin at the particle-level motion. To do so, we consider the particle-level reduced transverse VDOS, which determines how much each particle contributes to the reduced VDOS at a given frequency.

The results of this analysis are shown in Fig.3 for six different frequency values, from 0.4 to 12 Hz. A darker red indicates a more significant contribution to the reduced transverse VDOS at that frequency.

Panels (a)-(c) are for frequencies around the characteristic energy of the DFM, as indicated with the vertical gray region in Figs.1-2. In particular, panel (b) lies precisely at the frequency of the flat mode corresponding to the BP energy. In this range of frequencies, one-dimensional (1D) string-like structures emerge, indicating particles' heterogeneous dynamics and tendency to form collective excitations of approximately (1D) nature. These string-like dynamical defects are most substantial at the flat mode frequency, panel (b).

However, for higher frequencies, as shown in panels (d)-(f), the spatial distribution of the particle-level VDOS becomes more uniform, and no evident string-like structure is observed anymore. On the other hand, as shown explicitly in SI, the longitudinal particle-level VDOS does not display any string-like structure. This confirms the DFM's transverse nature and the localized string-like excitations.

To provide a stronger connection between the string-like defect structures, the BP anomaly in the VDOS and

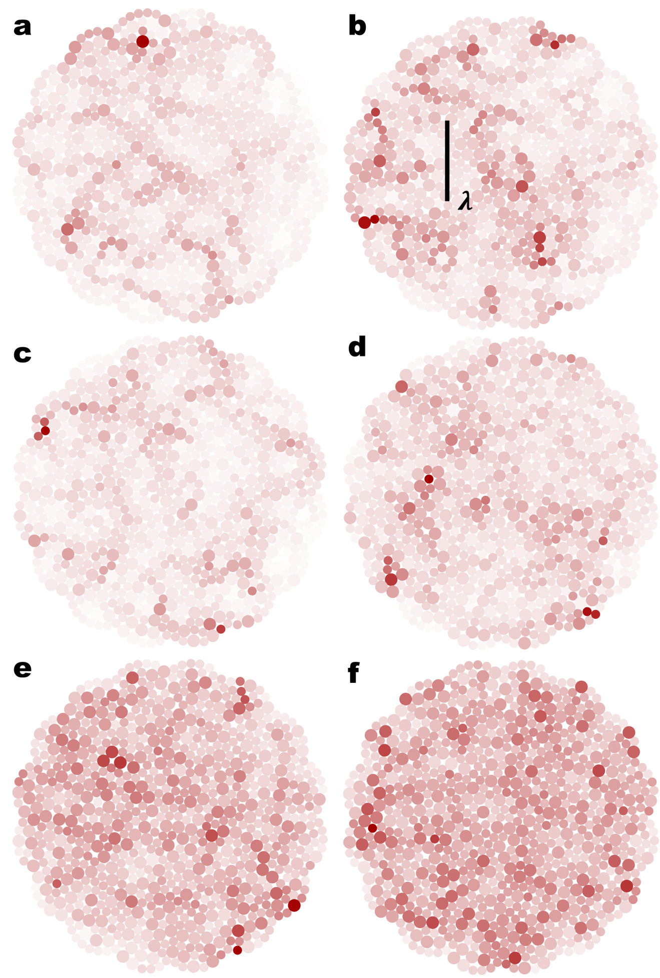

FIG. 3: The spatial distribution of transverse particle-level reduced VDOS at frequencies $0.4, 1.2, 2, 4, 8, 12$ Hz from panel **(a)** to **(f)**. A darker color indicates a more significant contribution to the reduced VDOS at a given frequency. The thick black line in panel (b) shows the extent of the average length of string-like dynamical defects, which is approximately $12d_s$.

the properties of the DFM, we follow the idea of associating a length scale with the boson peak introduced by Hong et al. [53, 54] and Kalampounias et al. [55] on a heuristic basis (see also [56–58]). We then define a cooperative length scale l,

$$l \approx \frac{v_T}{\omega_{BP}} = \frac{v_T}{\omega_{\text{DFM}}}, \tag{8}$$

whose value is determined up to an unknown $\mathcal{O}(1)$ coefficient. Using $\omega_{\text{DFM}} = \omega_{BP} \approx 2$ Hz, we find $l \approx 35\, d_s$. This value is approximately 3 times the average length of the string-like structures $\lambda \approx 12\, d_s$ observed in Fig.3.

This result is in qualitative agreement with recent theoretical studies [41, 42]. At zero temperature, or equivalently in the absence of damping, the length-scale l extracted from the BP and the average string-like defects length λ were found to match to a good approximation. In overdamped dynamics, the BP-like anomaly is softened by damping mechanisms, resulting in a longer length scale. As observed in glass-forming liquids above the glass transition temperature [41], in that case l is slightly larger than λ, consistent with our findings.

Finally, we notice that previous works connected the scale of dynamic heterogeneities ξ to the boson peak frequency, $\xi \approx c v_T/\omega_{BP}$, where c is a constant found to be between 1/2 and 1 [59–62, 62–64]. Therefore, our result suggests that the length-scale defined by the string-like defects is strongly related to the scale of dynamic heterogeneity, but possibly also to the scale defined by the fluctuations of the shear modulus or by low-energy quasi-localized structures, that are found to coincide in certain simulation glass models [65].

Conclusions– We conducted an experiment utilizing a quasi-two-dimensional disordered active Brownian particle system. Our investigation unveiled a robust correlation among a collective dispersionless flat mode, the boson peak anomaly in the vibrational density of states, and the emergence of string-like dynamical defects. Our findings affirm that string-like structures, predominantly of a transverse nature, may underlie the low-energy vibrational anomalies observed in active Brownian particles. This hypothesis was initially proposed in molecular glasses through simulations [38], and the existence of the boson peak aligns with a dispersionless localized mode, as evidenced experimentally in two-dimensional silica [44]. Our discoveries indicate striking parallels in the low-energy collective excitations of disordered active Brownian particles and molecular glasses, despite the myriad of distinctions between these systems.

Acknowledgments – We would like to thank Jack Douglas, Yunjiang Wang, Wensheng Xu, Haibin Yu, Peng Tan and Massimo Pica Ciamarra for numerous discussions about string-like objects and their role in amorphous systems. CJ and MB acknowledge the support of the Shanghai Municipal Science and Technology Major Project (Grant No.2019SHZDZX01). MB acknowledges the support of the sponsorship from the Yangyang Development Fund. ZZ, YC, and JZ acknowledge the support of the NSFC (No. 11974238 and No. 12274291) and the Shanghai Municipal Education Commission Innovation Program under No. 2021-01-07-00-02-E00138. ZZ, YC, and JZ also acknowledge the support from the Shanghai Jiao Tong University Student Innovation Center.

* Electronic address: b.matteo@sjtu.edu.cn
† Electronic address: jiezhang2012@sjtu.edu.cn

[1] M. C. Marchetti, J. F. Joanny, S. Ramaswamy, T. B. Liverpool, J. Prost, M. Rao, and R. A. Simha, Rev. Mod. Phys. **85**, 1143 (2013).
[2] M. E. Cates and J. Tailleur, Annual Review of Condensed Matter Physics **6**, 219 (2015).
[3] X. Zheng, B. ten Hagen, A. Kaiser, M. Wu, H. Cui, Z. Silber-Li, and H. Löwen, Phys. Rev. E **88**, 032304 (2013).
[4] F. Kümmel, B. Ten Hagen, R. Wittkowski, I. Buttinoni, R. Eichhorn, G. Volpe, H. Löwen, and C. Bechinger, Physical review letters **110**, 198302 (2013).
[5] C. Reichhardt and C. J. O. Reichhardt, Soft Matter **10**, 7502 (2014).
[6] S. Henkes, K. Kostanjevec, J. M. Collinson, R. Sknepnek, and E. Bertin, Nature communications **11**, 1405 (2020).
[7] A. R. Sprenger, M. A. Fernandez-Rodriguez, L. Alvarez, L. Isa, R. Wittkowski, and H. Lowen, Langmuir **36**, 7066 (2020).
[8] L. Caprini and H. Löwen, Physical Review Letters **130**, 148202 (2023).
[9] S. Bröker, J. Bickmann, M. Te Vrugt, M. E. Cates, and R. Wittkowski, Physical Review Letters **131**, 168203 (2023).
[10] K. Safferling, T. Sütterlin, K. Westphal, C. Ernst, K. Breuhahn, M. James, D. Jäger, N. Halama, and N. Grabe, Journal of Cell Biology **203**, 691 (2013).
[11] Y. Chen and J. Zhang, Phys. Rev. E **106**, L052903 (2022).
[12] Y. Chen and J. Zhang, arXiv preprint arXiv:2308.04219 (2023).
[13] A. Kudrolli, G. Lumay, D. Volfson, and L. S. Tsimring, Phys. Rev. Lett. **100**, 058001 (2008).
[14] V. Narayan, S. Ramaswamy, and N. Menon, Science **317**, 105 (2007).
[15] J. Deseigne, O. Dauchot, and H. Chaté, Phys. Rev. Lett. **105**, 098001 (2010).
[16] C. Scholz and T. Pöschel, Phys. Rev. Lett. **118**, 198003 (2017).
[17] C. Jiang, Z. Zheng, Y. Chen, M. Baggioli, and J. Zhang, "Experimental observation of gapped shear waves and liquid-like to gas-like dynamical crossover in active granular matter," (2024), arXiv:2403.08285 .
[18] P. Chaikin and T. Lubensky, *Principles of Condensed Matter Physics* (Cambridge University Press, 2000).
[19] B. I. H. P. w. Anderson and c. M. Varma, The Philosophical Magazine: A Journal of Theoretical Experimental and Applied Physics **25**, 1 (1972).
[20] W. A. Phillips, Journal of Low Temperature Physics **7**, 351 (1972).
[21] R. C. Zeller and R. O. Pohl, Phys. Rev. B **4**, 2029 (1971).
[22] E. Lerner and E. Bouchbinder, The Journal of Chemical Physics **155**, 200901 (2021).
[23] M. A. Ramos, *Low-temperature Thermal and Vibrational Properties of Disordered Solids: A Half-century of Universal" anomalies" of Glasses* (World Scientific, 2022).
[24] A. Argon, Acta Metallurgica **27**, 47 (1979).
[25] J. D. Eshelby and R. E. Peierls, Proceedings of the Royal Society of London. Series A. Mathematical and Physical Sciences **252**, 561 (1959).
[26] M. Baggioli, Nature Communications **14**, 2956 (2023).
[27] M. L. Falk and J. Langer, Annual Review of Condensed Matter Physics **2**, 353 (2011).
[28] H. Kleinert, *Gauge Fields in Condensed Matter: Vol. 1: Superflow and Vortex Lines (Disorder Fields, Phase Transitions) Vol. 2: Stresses and Defects (Differential Geometry, Crystal Melting)* (World Scientific, 1989).
[29] C. Donati, J. F. Douglas, W. Kob, S. J. Plimpton, P. H. Poole, and S. C. Glotzer, Phys. Rev. Lett. **80**, 2338 (1998).
[30] B. A. Pazmino Betancourt, J. F. Douglas, and F. W.

Starr, The Journal of Chemical Physics **140**, 204509 (2014).

[31] H. Zhang, X. Wang, H.-B. Yu, and J. F. Douglas, Journal of Chemical Physics **154**, 084505 (2021).

[32] H. Zhang, C. Zhong, J. F. Douglas, X. Wang, Q. Cao, D. Zhang, and J.-Z. Jiang, The Journal of Chemical Physics **142**, 164506 (2015).

[33] H. Zhang, M. Khalkhali, Q. Liu, and J. F. Douglas, The Journal of Chemical Physics **138**, 12A538 (2013).

[34] K. Zhao, M. Baggioli, W.-S. Xu, J. F. Douglas, and Y.-J. Wang, arXiv preprint arXiv:2402.10295 (2024).

[35] J.-H. Hung and D. S. Simmons, The Journal of Physical Chemistry B **124**, 266 (2020), pMID: 31886663.

[36] V. N. Novikov and N. V. Surovtsev, Phys. Rev. B **59**, 38 (1999).

[37] E. Bianchi, V. M. Giordano, and F. Lund, Phys. Rev. B **101**, 174311 (2020).

[38] Y.-C. Hu and H. Tanaka, Nature Physics **18**, 669 (2022).

[39] Y.-C. Hu and H. Tanaka, Phys. Rev. Res. **5**, 023055 (2023).

[40] H. Zhang, X. Wang, H.-B. Yu, and J. F. Douglas, The Journal of Chemical Physics **154**, 084505 (2021).

[41] C. Jiang, M. Baggioli, and J. F. Douglas, arXiv preprint arXiv:2311.04230 (2023).

[42] C. Jiang and M. Baggioli, arXiv preprint arXiv:2403.18221 (2024).

[43] J. Zhang, H. Zhang, and J. F. Douglas, The Journal of Chemical Physics **160**, 114506 (2024).

[44] M. Tømterud, S. D. Eder, C. Büchner, L. Wondraczek, I. Simonsen, W. Schirmacher, J. R. Manson, and B. Holst, Nature Physics **19**, 1910 (2023).

[45] C. R. Berardi, K. Barros, J. F. Douglas, and W. Losert, Phys. Rev. E **81**, 041301 (2010).

[46] H. Zhang, D. J. Srolovitz, J. F. Douglas, and J. A. Warren, Proceedings of the National Academy of Sciences **106**, 7735 (2009).

[47] K. H. Nagamanasa, S. Gokhale, R. Ganapathy, and A. K. Sood, Proceedings of the National Academy of Sciences **108**, 11323 (2011).

[48] S. Ramaswamy, Annu. Rev. Condens. Matter Phys. **1**, 323 (2010).

[49] A. Ghosh, V. K. Chikkadi, P. Schall, J. Kurchan, and D. Bonn, Phys. Rev. Lett. **104**, 248305 (2010).

[50] K. Chen, W. G. Ellenbroek, Z. Zhang, D. T. N. Chen, P. J. Yunker, S. Henkes, C. Brito, O. Dauchot, W. van Saarloos, A. J. Liu, and A. G. Yodh, Phys. Rev. Lett. **105**, 025501 (2010).

[51] V. Malinovsky, V. Novikov, and A. Sokolov, Physics Letters A **153**, 63 (1991).

[52] M. Baggioli, M. Vasin, V. Brazhkin, and K. Trachenko, Physics Reports **865**, 1 (2020), gapped momentum states.

[53] L. Hong, V. N. Novikov, and A. P. Sokolov, Phys. Rev. E **83**, 061508 (2011).

[54] L. Hong, V. Novikov, and A. Sokolov, Journal of Non-Crystalline Solids **357**, 351 (2011).

[55] A. G. Kalampounias, S. N. Yannopoulos, and G. N. Papatheodorou, The Journal of Chemical Physics **125**, 164502 (2006).

[56] V. Malinovsky, V. Novikov, A. Sokolov, and V. Bagryansky, Chemical Physics Letters **143**, 111 (1988).

[57] V. Malinovsky and A. Sokolov, Solid State Communications **57**, 757 (1986).

[58] A. J. Martin and W. Brenig, physica status solidi (b) **64**, 163 (1974).

[59] W. Schirmacher, B. Schmid, C. Tomaras, G. Viliani, G. Baldi, G. Ruocco, and T. Scopigno, physica status solidi c **5**, 862 (2008).

[60] E. Duval, A. Boukenter, and T. Achibat, Journal of Physics: Condensed Matter **2**, 10227 (1990).

[61] A. P. Sokolov, A. Kisliuk, M. Soltwisch, and D. Quitmann, Phys. Rev. Lett. **69**, 1540 (1992).

[62] S. R. Elliott, Europhysics Letters **19**, 201 (1992).

[63] B. Schmid and W. Schirmacher, Phys. Rev. Lett. **100**, 137402 (2008).

[64] A. Tanguy, J. P. Wittmer, F. Leonforte, and J.-L. Barrat, Phys. Rev. B **66**, 174205 (2002).

[65] S. Mahajan and M. P. Ciamarra, Phys. Rev. Lett. **127**, 215504 (2021).

Supplementary Information

In this Supplementary Information (SI), we provide further analysis on our experimental system.

The longitudinal dynamical structure factor as a function of frequency and for different wave-vectors is shown in Fig.S1. It can be fitted by a single damped harmonic oscillator function,

$$S_L(\omega, k) \propto \frac{\omega^2}{(\omega^2 - \Omega_L^2)^2 + \omega^2 \Gamma_L^2} \tag{S1}$$

that corresponds to an attenuated longitudinal phonon. The dispersion relation of this mode, indicated with a black dashed line in Fig.S1, is well approximated by a linear function $\Omega_L = v_L k$, with $v_L = 116.9$ d_s/s.

In Fig.S2, we present the particle level longitudinal vibrational density of states. Contrary to the transverse component discussed in the main text, we do no observe any clear evidence of string-like dynamical defects.

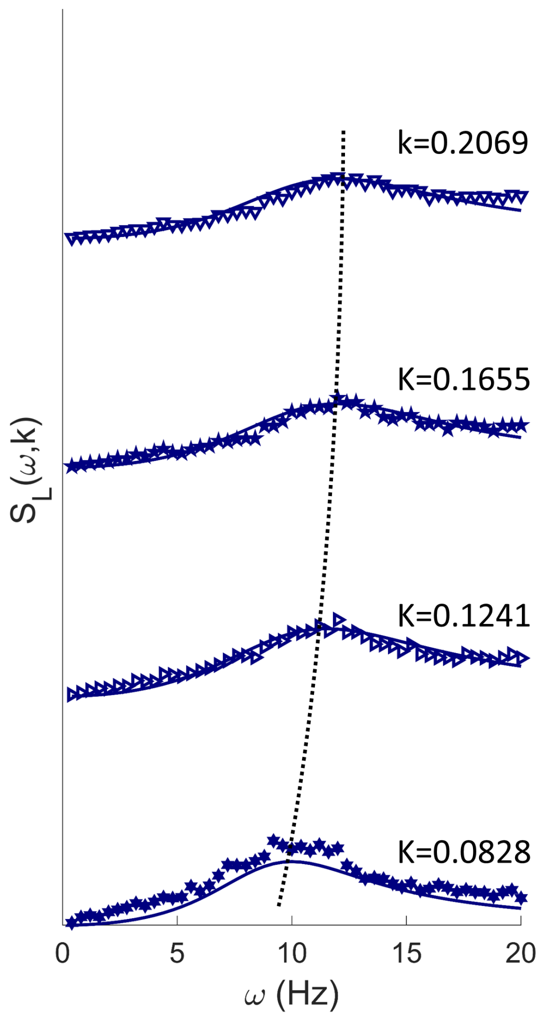

FIG. S1: The longitudinal dynamical structure factor $S_L(\omega, k)$ as a function of the frequency for different wave-vectors (labeled in figure). The solid lines indicate the fit to the damped harmonic oscillator function, Eq. (S1). The black dashed line indicates the dispersion of the longitudinal mode $\Omega_L(k)$.

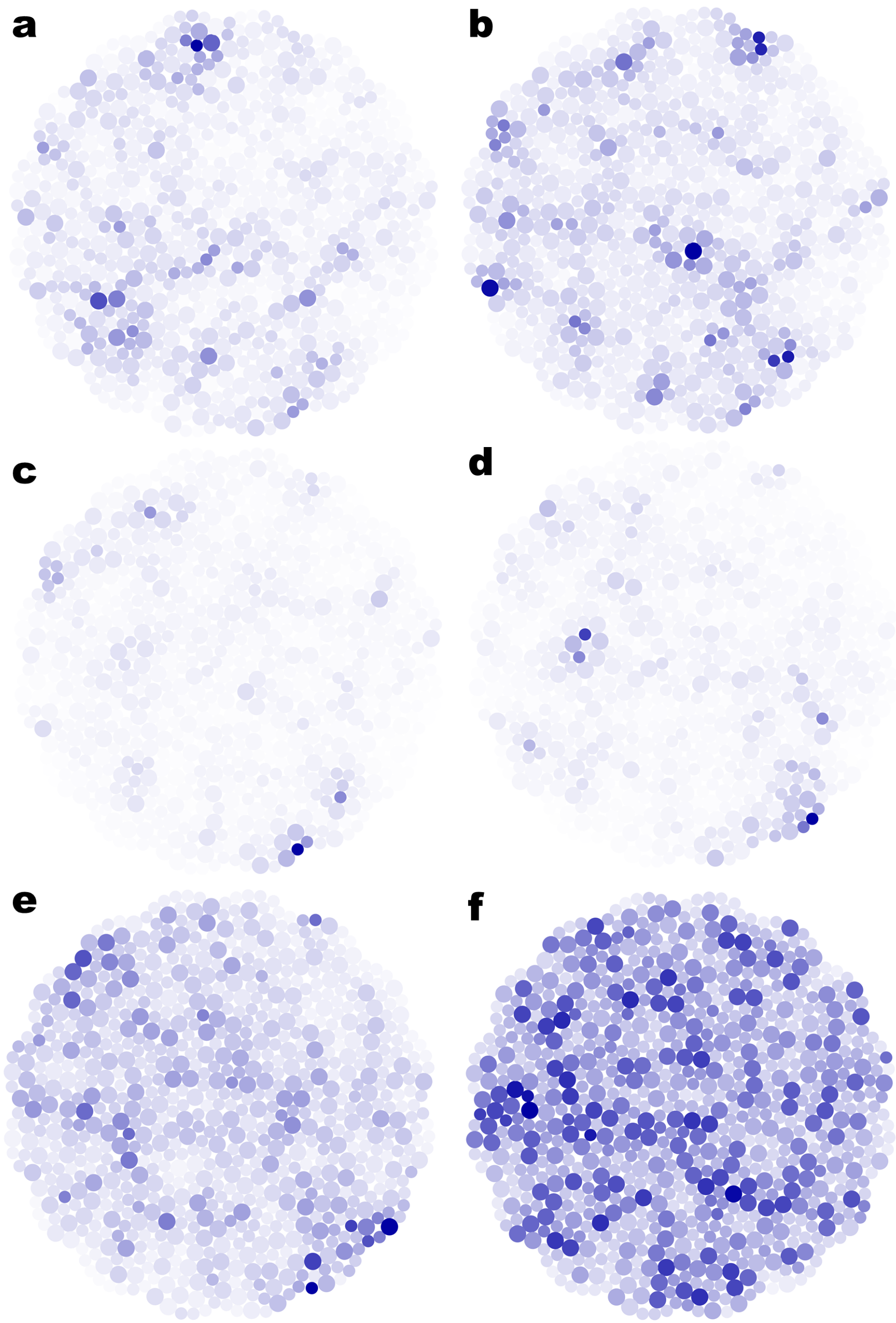

FIG. S2: The distribution of longitudinal particle level VDOS with frequency $0.4, 1.2, 2, 4, 8, 12$ Hz from panel **(a)** to **(f)**. The darker color the more contribution of the particle to VDOS.